A Broadband Laser Illuminator for Active Hyperspectral Imaging

Agustin I. Ifarraguerri, Leidos, Arlington, VA

Mohammed N. Islam, Larry Peterson, Kevin Ke, Mike Freeman, Omni Sciences, Dexter, MI

Joseph Meola, Anthony Absi, James Leonard, Air Force Research Laboratory, WPAFB, OH

ABSTRACT

We have been investigating the use of supercontinuum (SC) laser technology to provide active illumination for shortwave infrared (SWIR) hyperspectral sensors in order to extend their operational window into the night and heavy overcast periods. Unlike a lamp, light from a broadband laser illuminator (BLI) can propagate long distances through the atmosphere while maintaining its spatial coherence as well as high power efficiency. BLI sources have been demonstrated covering the SWIR spectral windows from 1µm to 2.5µm. We recently tested a compact source capable of producing 64W of SC output in the 1-1.8µm spectral region with 15% wall-plug efficiency. We also demonstrated end-to-end sensing with a SWIR hyperspectral camera at a distance of 1.4km on a slant path near the ground. An average signal-to-noise ratio (SNR) of 126 against sensor dark noise was achieved when the beam was spread across a few pixels on a reflective target. An operationally useful system will need the beam to be spread over tens of square meters. Achieving good SNR in this case will require higher output power, which may be achieved by combining multiple sources, as well as hyperspectral cameras (receivers) with high optical efficiency and very low-noise.

Keywords: broadband laser illuminator, supercontinuum laser, hyperspectral imaging

1. INTRODUCTION

Although hyperspectral imaging (HSI) has been of interest to the DoD and the intelligence community for many years, its operational utility has remained limited in part by the requirement for solar illumination at the shorter wavelengths (visible, near-IR and SWIR). Useful HSI data requires sun angles available for no more than 7 hours each clear day, depending on the location and time of year. Cloud cover also reduces illumination and restricts the utility of the HSI data. Moving beyond these limitations requires active illumination, which can extend the operational envelope of the technology to 24 hours. Additional advantages of active illumination include the elimination of shadows (when the source and receiver are co-located) which alter the measured spectral signature and increase false alarms, improved change detection by providing a consistent illumination geometry, retrieval of surface reflectance at short ranges, and the possibiliy of range gating with modulated sources that would allow ranging and forest canopy penetration.

Previous attempts at active HSI illumination have focused on laser sources at selected wavelengths, but this approach gives up a great deal on information at wavelengths that are not illuminated. In the late 1990's, researchers at MIT's Lincoln Laboratory built two prototype imaging spectrometers using "white light" lasers that took advantage of the stimulated Raman scattering (SRS) effect [1,2]. However they were not able to move beyond the laboratory due to the low available laser output power. More recently, a 25-band laser detection and ranging (LADAR) system was demonstrated [3] capable of up to 40m range. With the rapid advances in high-power diode laser pumps, it has now become possible to develop a broad-band laser illuminator (BLI) based on super-continuum (SC) laser technology with sufficient intensity at range to match the sunlight. Our development efforts have concentrated in the SWIR region of the spectrum, but this technology is applicable in the visible and in the mid-wave infrared.

2. SUPERCONTINUUM LASER DEVELOPMENT AND TESTING

There are two possibilities for illuminating a surface for spectral interrogation: lamps and lasers. Lamps can produce smooth, broad-band illumination that can be customized by optical filtering, but to maintain brightness at multi-kilometer ranges the beam needs to be highly collimated and spatially coherent, neither of which have been efficiently achieved with lamps thus far. Lasers, on the other hand, have the correct spatial characteristics to deliver high brightness at a distance, but have been limited in wavelength range.

SC lasers are the first technology to successfully combine broadband characteristics with laser spatial performance. To create a "super-continuum" output in a spatially coherent laser, a diode laser output is optically amplified and used to pump a short length of highly nonlinear optical fiber (Figure 1). Use of modulation instability and stimulated Raman scattering in the fiber enables the use of compact laser diodes as the primary source of energy while maintaining spatial coherence [4]. SC generation has been demonstrated at wavelengths as short as 0.35μm and as long as 4.5μm [5], and extension to 5.5μm is possible with new indium fluoride fibers.

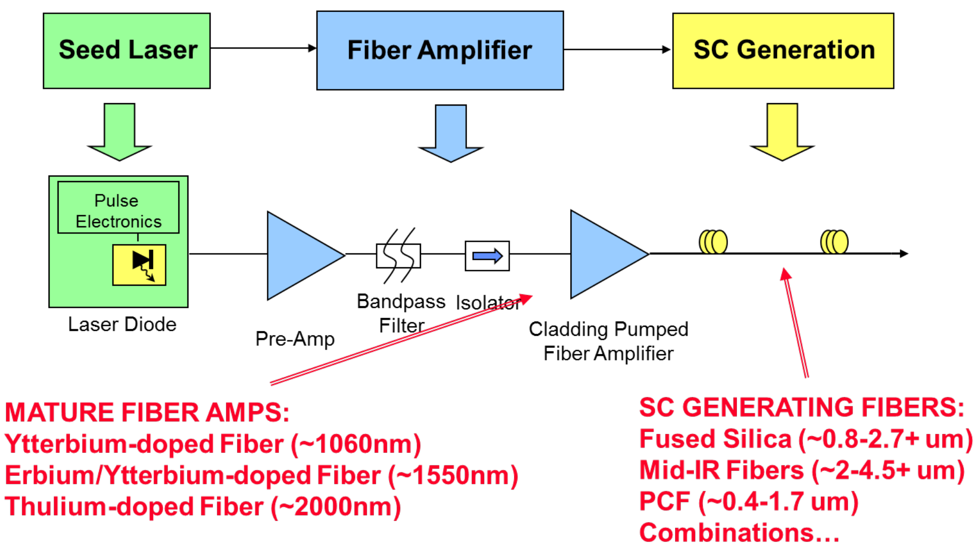

Figure 1: Top-level SC generation design using all-COTS components.

A combination of SC lasers could be used to cover the entire solar reflective spectral region (0.4-2.5μm wavelengths), but for covertness, eye safety and mission relevance it makes sense to start in with the SWIR region, from 1μm to 2.5μm. Mature fiber optic amplifier options for this spectral band include Erbium/Ytterbium-doped fiber amplifiers for SC in the 1μm to 2μm band, and Thulium-doped fiber amplifiers for SC in longer wavelengths out to 2.5μm. Once a SWIR system has proven successful, the wavelength range can be extended to the near-infrared and visible regions, while maintaining operational eye safety.

Initial calculations showed that to match sunlight, it would be necessary to generate at least 50-100 Watts per micron per square meter, so we set a goal of SC output power density of 100W/µm as the initial benchmark. In 2012, we built and tested a Thulium-based laboratory prototype in the 2-2.5µm region with 25W of SC output, or 50W/µm [6]. Figure 2 shows the radiance spectrum produced by the 25W breadboard as measured against a Spectralon™ target at one meter from the source, as compared to an equivalent measurement with solar illumination at a 50° elevation (40° zenith angle).

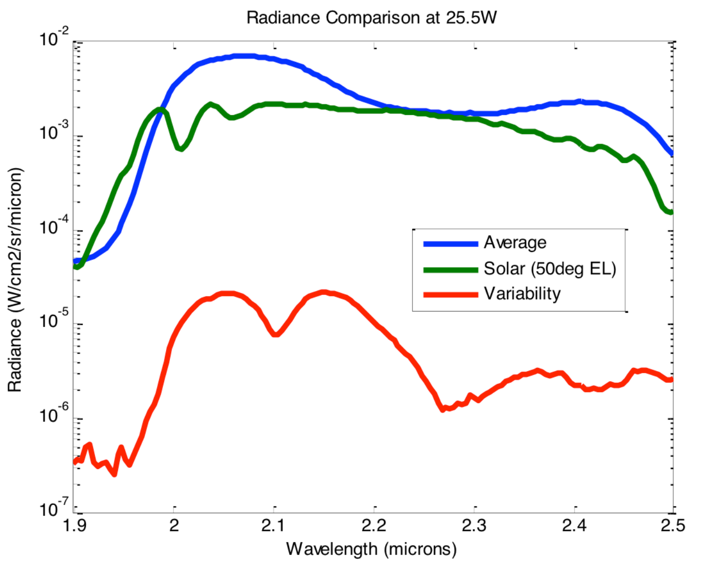

Figure 3: Average radiance and variability measured from 25W breadboard source as reflected from Spectralon at 1 meter from the source. Equivalent solar radiance is shown for comparison.

This experiment demonstrated the feasibility of generating high power. It was shown that the fused silica SC fiber generates a diffraction-limited single mode with beam shape metric $M^2<1.2$ and an output stability of <0.7% over periods of seconds to minutes. We performed spectral reflectance measurements to illustrate the overall concept and showed good agreement with conventional measurements with lamps. Because the 25W prototype was a laboratory experiment, we developed a second source for field testing of the concept and to help characterize the atmospheric propagation of the beam. The field source (Figure 3) covered the spectral range of 1.5-2.3µm with a total output of 5W (corresponding to ~6.25W/µm). We were able to propagate the beam from the 76m-tall AFRL tower at Wright-Patterson Air Force Base to a 2.5m ground-based target at 1.6km slant range. The beam characteristics were measured at ground levelas well as the spectral reflectance of various surfaces [7].

Figure 2: 5W BLI field prototype

Having demonstrated high-power SC generation as well as beam propagation, in 2013 we developed a new prototype in the 1-1.8µm region with a goal of 50W total output power (62.5W/µm) and high wall-plug efficiency (Figure 4). Using Ytterbium power amplifiers, we were able to achieve a total of 64W output power (80W/µm) at better than 15% wall-plug efficiency, which is within 20% of our original benchmark. The 2013 prototype was tested at the AFRL tower with the ground-based target at a 1.4km slant range and a hyperspectral camera co-located with the source. The slightly shorter distance was chosen to mitigate the effects of the atmospheric turbulence on the beam which is primarily an artifact of the experiment geometry and not necessarily an operational limitation. The beam was directed from the tower through 7 relay mirrors to the 2.5m target where it created a 90cm spot. Because of mirror losses, the maximum output from the

Figure 4: 50W BLI field prototype

tower was ~55W. The HSI receiver was a commercial system from Headwall Photonics with sensitivity from 1-2.5µm. A 100mm lens was used in the experiment, providing a ground sample distance (GSD) of 42cm. Most of the laser signal was contained in a 3x3 pixel cluster. No beam shaping was attempted, though this may be necessary in the future to optimize the light field. The test results are described in more detail in [8]. This was the first-ever experiment of two-way propagation of the active HSI illumination over a long distance, and demonstrated the feasibility of the overall concept.

Figure 5 shows the average radiance signal measured by the Headwall spectrometer, compared to the signal variability induced mostly by atmospheric turbulence and to the sensor dark noise-equivalent spectral radiance (NESR). The signal is two orders of magnitude above the dark noise but only ~10x the total variability, which includes the effect of turbulence. This is an unfortunate result of the test configuration. To show this, we can use the Tatarski approximation of the change in turbulence strength with altitude near the ground [9]:

$$C_n^2 \approx C_{n0}^2 h^{-4/3},$$

where C_{n0}^2 is the refractive index structure function coefficient near the ground and h is the height above the ground in meters. By integrating over the line of sight, we can estimate the total expected turbulence effect along the slant path, which results in the formula:

$$C_n^2(R,\theta) = 3C_{n0}^2(\sin\theta)^{-4/3}\left[\left(\frac{h_0}{\sin\theta}\right)^{-1/3} - \left(\frac{h_0}{\sin\theta} + R\right)^{-1/3}\right],$$

where R is the slant range to the target, θ is the depression angle, and h_0 is the height of the target above the ground (assumed to be 1 meter in this case). Using this expression we can compare the experiment scenario (θ=3.15° and R=1,400m) to a nadir geometry (θ=90°) for the same atmospheric state. We find that at 3000m altitude (~10,000') looking nadir, the turbulence effect is approximately 1/15th of that seen at the tower test. From this we can estimate that the ~10% radiometric variability measured at the test would be around 0.7% at nadir, and thus the SNR would be dominated by dark and shot noise. Because the atmospheric turbulence strength decays very rapidly with altitude, this result does not change significantly at higher altitudes.

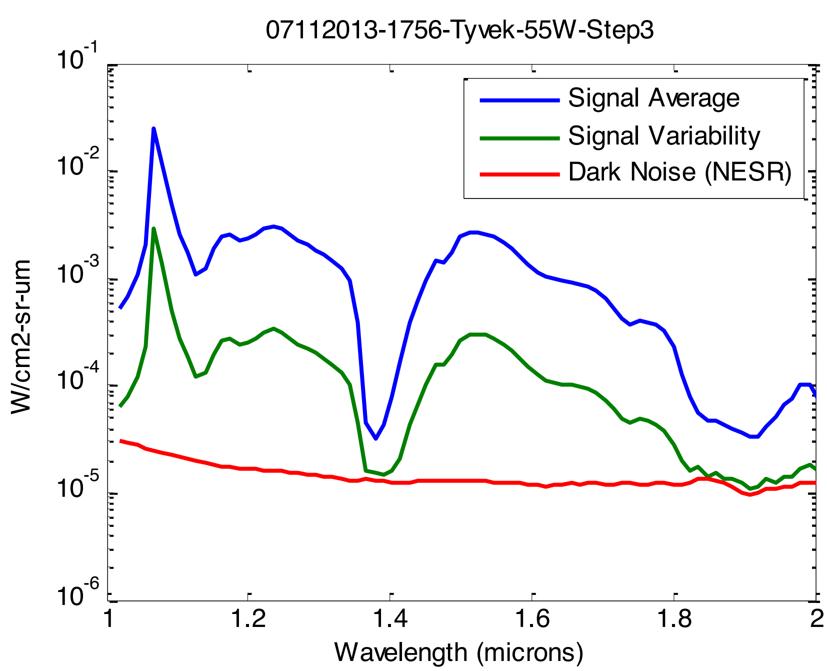

Figure 5: Measured average radiance, radiance variability and sensor noise for 2013 field experiment at 1.4km slant range.

3. SYSTEM PERFORMANCE MODEL

In parallel with the development of the BLI, system-level radiometric performance models have been developed by Leidos and AFRL to gain an understanding of the capabilities and limitations of the source and to drive requirements. Both models consider the full sensing scenario including the geometry, source emission, atmosphere, target, and receiver design. A description and results from the ARFL model was recently reported by Meola *et al* [8]. The Leidos version is briefly described here.

The modeling chain begins with the measured BLI source emission power spectral density as measured in the lab. The atmospheric transmission is modeled with MODTRAN and the target is characterized by a backscatter reflectance factor which is assumed to be equal to the diffuse reflectance of the material. The hyperspectral receiver is assumed to image a slit that is scanned along one direction to form an image. The optical characteristics of the receiver include the optics F/#, number of spatial detectors along the slit, detector field of view, detector size, quantum efficiency, optical efficiency, spectral band-width, detector dark current, and read noise. The model does not (yet) account for near-field backscatter, the non-square shapes of the source laser beam or receiver point spread function.

System-level parameters include area coverage rate, altitude (or range), and boresight efficiency (the percentage of reflected light that is actually captured by the receiver). Unlike with passive sensors, the SNR performance of an active system is dependent on the area that is illuminated since a finite amount of power must be spread over the area. Increasing the area coverage rate by making the imaging footprint larger decreases the irradiance and therefore the signal. There are multiple implementations of the same basic model for different scenarios. Some include platform and scanning mirror motion to derive geometry. Here we show some example results assuming an area coverage rate independent of the platform.

Although the model has not been formally validated, we compared the results with the measurements from the 2013 experiment. Several of the receiver parameters such as the optical efficiency, quantum efficiency and detector dark noise (dark current + read noise) were unknown to us so we used reasonable assumptions based on experience and adjusted them to match the calibration and noise measurements made with a calibrated integrating sphere. Under these conditions the model predicted the received radiance at the aperture to within 12% on average. From this point we can extrapolate from the measured SNR of 126 relative to dark noise to a mean total SNR of 79 that includes the shot noise from the signal. The background-limited (BLIP) SNR under these conditions is 229.

The model allows us to trade key parameters, particularly SNR versus area coverage rate and BLI output power. Figure 6 shows such a graph of average SNR over the 1-1.8μm band. The system was modeled with 0.5m pixels at a 3000m range. The receiver was assumed to have an F/# of 2.4 with 320 pixels at 40μm pitch, optical efficiency of 40%, average quantum efficiency of 80%, and boresight efficiency of 80% as well. The dark noise per pixel was assumed to be 200 electrons which includes both dark current and read noise. The ground reflectance was set at 25% and the FWHM spectral bandwidth was 12.5nm. Three BLI output power levels are modeled. The SNR predictions show that at 100W/μm (which is expected to be achieved in the near term), we can scan 10^4 square meters per second with SNRs comparable to those of passive HSI sensors. However, to match the area coverage rates of these airborne sensors (~10^5 square meters per second), we will need output power densities of 500W/μm or even 1000W/μm, depending on the sensing scenarios and the capabilities of the receiver. Increasing power to these levels is feasible but will require progressively aggressive thermal management and improved efficiency. At the current 15% wall-plug efficiency, a 500W/μm output over the 1-2.5μm range would require 5kW of input power. Approaches to increasing output power include increasing optical amplifier gains (up to the SC fiber damage threshold), fiber bundling, or simply combining multiple separate BLI units.

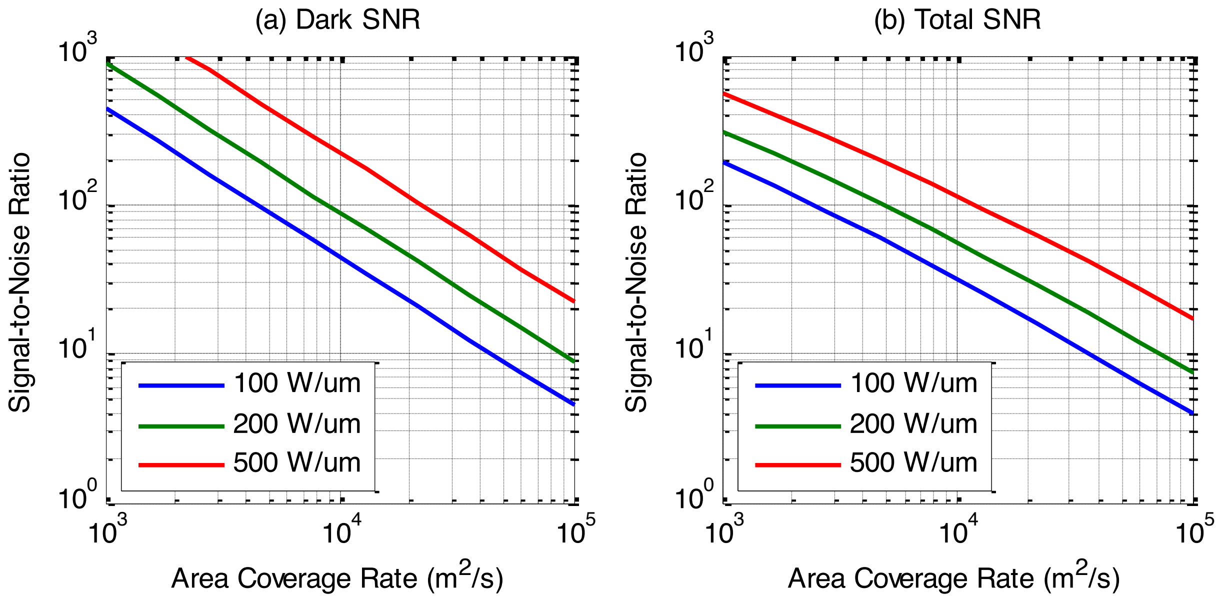

Figure 6: Model average SNR predictions vs. area coverage rate at 3 power densities for example system with 0.5m pixels at 3000m.

4. SUMMARY & FUTURE STEPS

We have outlined the development of a BLI appropriate for use with hyperspectral sensors in both ground-based and airborne sensing. Our initial goal of 100W/µm output is well within reach and scaling up to higher output power can be achieved by increasing amplifier gains, bundling fibers and using multiple units. There are several ways to combine multiple sources into a single output. Sources covering different spectral bands can be combined using a wavelength-division multiplexing (WDM) technology. For increasing power by bundling, an array or apertures can be constructed that can provide a light field of the desired shape. This approach mitigates thermal management challenges by maintaining physical separation of the fibers which allows for effective heat conduction strategies. The payoff is multi-fold. Aside from the ability to operate VNIR/SWIR HSI at night and under heavy clouds, there is potential to fundamentally improve change detection and to exploit the pulsed nature of the source to provide hyperspectral LADAR.

Change detection is improved by providing a constant illumination source with consistent geometry so that algorithmic compensation for changing sun angle and illumination color is not necessary. To use a BLI in this way during the day, it is necessary to "turn off the sun", which can be achieved by modulating the source at a frequency high enough to "freeze" the background illumination and allow for subtraction. This is a near-term development effort for the program.

The Omni BLI sources have typical pulse repetition frequencies (PRF) in the single MHz range. At these PRFs the range ambiguity for topographic LADAR applications is significant (100 meters at 3MHz). To overcome this limitation, we can use encoded modulation schemes using pseudorandom sequences that allow correlation of the signal with no range ambiguity. This technique is currently applied to aerosol backscatter LADAR but can be extended to topographic applications.

We have demonstrated the feasibility of this concept with ground and tower-based experiments. The next logical step is to develop a flight-capable source that can be tested with an HSI receiver. Demonstrating airborne operation does not require building a full-scale system. Only a few pixels need be illuminated to show feasibility.

ACKNOWLEDGEMENTS

This work was performed under Air Force contract FA8650-12-D-1344. The authors would like to thank Mike Wager, Erica Whitfield, John Smotherman and Tyler Masterson for their excellent support during the test. We also extend our appreciation to the National Geospatial Intelligence Agency (NGA) for use of the Headwall hyperspectral camera and the FLIR6702 camera.

REFERENCES

1. B. Johnson, R.M. Joseph, M.L. Nischan, A. Newbury, J.P. Kerekes, H. Barclay, B. Willard and J.J. Zayhowski, “A compact, active hyperspectral imaging system for the detection of concealed targets,” *SPIE* 3710, 144-153 (1999)

2. M.L. Nischan, R. M. Joseph, J.C. Libby, and J.P. Kerekes, “Active Spectral Imaging,” *Lincoln Lab. J.* 4(1), 131-144 (2003)

3. M.A. Powers and C.C. Davis, “Spectral LADAR: active range-resolved three-dimensional imaging spectroscopy,” *Applied Optics* 51(10), 1468-1478 (2012)

4. C. Xia, M. Kumar, M.Y. Cheng, O. P. Kulkarni, M. N. Islam, A. Galvanauskas, F. L. Terry, Jr., M. J. Freeman, D.A. Nolan and W.A. Wood " Supercontinuum Generation in Silica Fibers by Amplified Nanosecond Laser Diode Pulses," *IEEE Journal of Selected Topics in Quantum Electronics*, 13(3), 789-797 (2007)

5. C. Xia, M. Kumar, O.P. Kulkarni, M.N. Islam, F.L. Terry, M.J. Freeman, M. Poulain, and G. Mazé, "Mid-infrared supercontinuum generation to 4.5 μm in ZBLAN fluoride fibers by nanosecond diode pumping," *Optics Letters* 31, 2553-2555 (2006)

6. V.V. Alexander, Z. Shi, M.N. Islam, K. Ke, M.J. Freeman, A. Ifarraguerri, J. Meola, A. Absi, J. Leonard, J. Zadnik, A.S. Szalkowski and G.J. Boer, “Power scalable >25 W supercontinuum laser from 2 to 2.5 μm with near-diffraction limited beam and low output variability,” *Optics Letters* 38(13), 2292-2294 (2013)

7. V.V. Alexander, Z. Shi, M.N. Islam, K. Ke, G. Kalinchenko, M.J. Freeman, A. Ifarraguerri, J. Meola, A. Absi, J. Leonard, J. Zadnik, A.S. Szalkowski and G.J. Boer, “Field trial of active remote sensing using a high-power short-wave infrared supercontinuum laser,” *Applied Optics* 52(27), 6813-6823 (2013)

8. J. Meola, A. Absi, M.N. Islam, L. Peterson, K. Ke, M.L. Freeman and A. Ifarraguerri, “Tower testing of a 64W shortwave infrared supercontinuum laser for use as a hyperspectral imaging illuminator,” *SPIE* 9088, 9088-1 – 9088-11 (2014)

9. V. I Tatarski, *Wave Propagation in a Turbulent Medium*, McGraw-Hill, New York (1961)